

Hyperfine coupling in singlet ground state magnets

Peter Thalmeier

Max Planck Institute for Chemical Physics of Solids, D-01187 Dresden, Germany

(Dated: December 19, 2025)

The influence of hyperfine coupling to nuclear spins and of their quadrupolar splitting on the induced moment order in singlet ground state magnets is investigated. The latter are found among non-Kramers f electron compounds. Without coupling to the nuclear spins these magnets have a quantum critical point (QCP) separating paramagnetic and induced moment regime. The hyperfine interaction suppresses the QCP and leads to a gradual crossover between induced electronic and nuclear hyperfine coupling dominated magnetic order. It is shown how the critical temperature depends on the electronic and nuclear control parameters including the nuclear spin size and its possible nuclear quadrupole splitting. In particular the dependence of the specific heat on the control parameters and applied field is investigated for ferro- and antiferromagnetic order. It is shown that the three peak structure in the electronic induced moment regime gradually changes to a two-peak structure in the hyperfine coupling dominated nuclear moment order regime or for increasing field strength. Most importantly the possibility of a reentrance behaviour of magnetic order or likewise nonmonotonic critical fields due to hyperfine coupling influence is demonstrated. Finally the systematic evolution of the phase diagram under the influence of nuclear quadrupole coupling is clarified.

I. INTRODUCTION

The common picture of semiclassical magnetism involves ions with a degenerate spin or pseudospin ground state which carry free magnetic moments in the paramagnetic state. They then order spontaneously due to intersite interactions at the magnetic transition temperature [1]. The size of the ordered saturation moment will be reduced from the classical value by the effect of quantum fluctuations and possibly by geometric or interaction frustration [2]. This simple picture is applicable to numerous compounds with transition elements, in particular the 4f-based materials. For these the presence of the crystalline electric field (CEF) plays an essential role. For half integer total angular momentum J of the 4f ions the ground state has always Kramers degeneracy implying picture of semiclassical order may be used, except in the quasi-one dimensional case. But for integer J non-Kramers ions such as Pr, Tm, Tb a distinct possibility arises because the CEF ground state may be a singlet $|0\rangle$ that is *nonmagnetic*, i.e. $\langle 0|J|0\rangle = 0$, preventing the application of the quasiclassical theory of magnetic order. However, if there is a close by excited state e.g. another nonmagnetic singlet $|1\rangle$ the two states can be connected by a finite nondiagonal matrix element $m_s = \langle 0|J_z|1\rangle$ of a total angular momentum component. Then the intersite exchange of CEF states may spontaneously mix the two states and thus induce a moment in the superposition ground state of $|0\rangle, |1\rangle$ that forms below the induced moment ordering temperature. In this mechanism the creation and ordering of moments happens simultaneously at the transition temperature. Literally this picture of induced moment order applies if the other CEF states happen to lie at much higher energy. Furthermore the first excited state does not have to be necessarily another singlet but may also be a doublet or triplet, depending on CEF site symmetry and still the induced moment mechanism is involved [3]. It is also possible that higher order multipole moments like quadrupoles [4] or hexadecapoles [5] may appear in this way.

Close to the QCP where the induced ground state moment collapses with a square root singularity [3] the ordering is nat-

urally very sensitive to external perturbations like magnetic field [6] or pressure [7]. A similar sensitivity is caused by further internal interactions like the hyperfine coupling to nuclear spins and the splitting of the latter originating from a nuclear quadrupole potential. Mostly these nuclear hyperfine effects have been investigated for 4f magnetic compounds with Kramers ground state ions like Ce or Yb [8–12] or non-Kramers ions with degenerate ground states like Pr [13] or Ho [14] cage compounds. By applying magnetic fields the ordered phases of such compounds may be tuned to quantum critical points which are also influenced by the presence of hyperfine coupling effects[15].

The hyperfine interaction may indeed be strong for some of the non-Kramers ions which have possible CEF singlet ground states, depending on local site symmetry and CEF potential of the 4f compound in which they appear. These ions and some of their essentials, including the strength of hyperfine couplings are listed in Table I. Their importance for compounds where non-Kramers RE ions have a nonmagnetic singlet ground state has in fact been known for some time [7, 16–21] and has gained renewed attention more recently [22–24]. In particular concerning the magnetocaloric properties and anomalous critical field dependence on temperature which may be interpreted as reentrance of multipolar or magnetic order. The latter effect has also been seen in Kramers ion Yb compounds [11] for magnetic order and was attributed to the effect of hyperfine coupling.

In this work we investigate in detail how the hyperfine coupling and quadrupolar splitting of nuclear spins can be included in the induced moment mechanism for singlet ground state magnets. We reconsider the phase diagram as function of electronic (CEF) and nuclear control parameters and discuss how the QCP is suppressed by the nuclear interactions and changed into a gradual crossover from CEF exchange dominated induced moment magnetism to hyperfine coupling dominated nuclear magnetism. We also show that the crossover between these regimes is quite sensitive to the sign and size of the nuclear quadrupole interaction. Particular attention is given to the specific heat anomalies that have both electronic

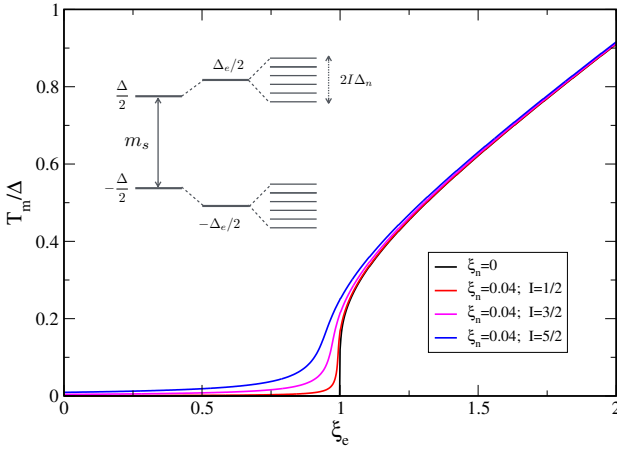


FIG. 1. Critical temperature T_m for induced magnetic order (FM or AFM) as function of electronic control parameter ξ_e for fixed nuclear ξ_n and three different sizes of nuclear spin I . The black line corresponds to vanishing hyperfine coupling when induced order appears only above the QCP at $\xi_e = 1$ (Eq. (15)). For finite hyperfine coupling ξ_n also T_m is finite for any ξ_e . This leads to a suppression of the QCP which becomes more pronounced with increasing nuclear spin size. The inset is a schematic view of the repulsion and splitting of electronic and nuclear levels ($I=5/2$) in the ordered regime.

CEF and nuclear contributions. It is demonstrated that depending on the location of control parameters a triple peak or double peak structure of the specific heat is expected as function of temperature. Furthermore we discuss the magnetic field dependence of specific heat of singlet ground state ferro- (FM) and antiferromagnetic (AFM) cases with nuclear spins involved and identify their characteristic signatures on both sides of the QCP. Most importantly we show that for the AFM case the coupled system of split electronic singlets and nuclear spins leads to a reentrance of magnetic order as function of temperature for high fields. This observation and the equivalent anomalous critical field dependence on temperature is a direct consequence of the hyperfine coupling.

II. HYPERFINE COUPLING FOR SINGLET GROUND STATE INDUCED MOMENT SYSTEMS

For investigating the effect of nuclear hyperfine coupling on induced electronic magnetic order and the resulting signatures in the specific heat we use the most simple and yet illustrative and experimentally relevant singlet-singlet model coupled to nuclear spins (nSSM), consisting of transverse Ising type electronic part and concomitantly an Ising type nuclear hyperfine coupling term. It is a nuclear-spin extension of the induced moment model investigated previously [3, 6] for various thermodynamic and dynamic properties.

The electronic states consist of two slightly split CEF singlets $|0\rangle$ and $|1\rangle$ at energies $\pm\Delta/2$, respectively, where Δ is the splitting energy. They may originate as low lying states for non-Kramers ions with total angular momentum $J = 4, 6$ which are split off from the group of higher lying states by a

suitable crystalline electric field. As an example we can have such non-Kramers quasi-doublet in a uniaxial CEF (e.g. D_{4h} symmetry) for total angular momentum $J=4$. Then the SSM corresponding to a D_{4h} representation may be given in terms of free ion states $|J, M\rangle \equiv |M\rangle (|M| \leq 4)$ by

$$\begin{aligned} |0\rangle &= \cos \alpha |0\rangle + \sin \alpha \frac{1}{\sqrt{2}} (|+4\rangle + |-4\rangle) \quad (\Gamma_1^{(1)}) \\ |1\rangle &= \frac{1}{\sqrt{2}} (|+4\rangle - |-4\rangle) \quad (\Gamma_2) \end{aligned} \quad (1)$$

This Ising-type SSM is relevant for Pr compounds [3, 7] with uniaxial symmetry and has also been applied to U- compounds [25–27]. The mixing angle α is determined by the CEF parameters. The Ising moment operator $J_z = m_s S_x$ in pseudo spin representation within this subspace where $m_s = \langle 0 | J_z | 1 \rangle = 8 \sin \alpha$ is then given by

$$J_z = \frac{m_s}{2} \begin{pmatrix} 0 & 1 \\ 1 & 0 \end{pmatrix} = m_s S_x; \quad (2)$$

where \mathbf{J} -operators refer to the free $|JM\rangle$ states and \mathbf{S} are the pseudo-spin operators in the reduced subspace of CEF singlet states. We note that a singlet-singlet level scheme in a uniaxial symmetry is not able to support an xy-type SSM. An inspection of the point group multiplication tables leads to the conclusion that this is forbidden for any symmetry [3].

The nuclear spin states $|II_z\rangle \equiv |I_z\rangle$ of the magnetic ion with spin size I form a $(2I+1)$ -fold degenerate multiplet. It will be split in the magnetically ordered phase due to the action of molecular field mediated by the hyperfine coupling with a strength given by the constant A in Table I, i.e. assumed to be positive. Later we also include possible single site nuclear quadrupole terms which will also split the nuclear multiplet. We do not consider the effect of long range nuclear dipole interactions.

The nuclear extended nSSM in pseudospin representation is then defined by the Hamiltonian

$$\begin{aligned} H &= \Delta \sum_i S_{zi} - m_s^2 I_0 \frac{1}{2} \sum_{\langle ij \rangle} S_{xi} S_{xj} \\ &+ A \sum_i S_{xi} I_{zi} - m_s h \sum_i S_{xi} \end{aligned} \quad (3)$$

where the first term is the CEF splitting, the second one the effective (N.N.) intersite exchange of 4f-pseudospins the third one is the hyperfine coupling which is also necessarily of Ising type since $S_{x,y}$ components are absent in the two-singlet space of Eq. (1). The last term is the Zeeman energy of electronic states in external field \mathbf{H} with $h = g_J \mu_B H$. The direct Zeeman term of nuclear spins is not included due to the much smaller nuclear magneton $\mu_n \ll \mu_B$. Note we use the convention I_0 positive or negative for FM or AFM exchange, respectively, while $A > 0$ means the electronic and nuclear spins are oriented oppositely.

In molecular field approximation (MFA) we then have $H_{mf} = \sum_{i\lambda} h_{mf}^\lambda(i)$ with

$$\begin{aligned} h_{mf}^\lambda(i) &= \hat{h}_{mf}^\lambda(i) + \frac{1}{2}\sigma m_s^2 I_e \langle S_x \rangle_\lambda \langle S_x \rangle_{\bar{\lambda}} - A m_s \langle S_x \rangle_\lambda \langle I_z \rangle_\lambda \\ \hat{h}_{mf}^\lambda(i) &= \Delta S_z(i) - m_s h_e^\lambda S_x(i) + h_n^\lambda I_z(i), \end{aligned} \quad (4)$$

Here $\lambda = A, B$ ($\bar{\lambda} = B, A$) denotes the sublattices in the case of AFM order with $\langle S_x \rangle_{\bar{\lambda}} = -\langle S_x \rangle_\lambda$ and likewise $\langle I_z \rangle_{\bar{\lambda}} = -\langle I_z \rangle_\lambda$ for zero field. The sublattice index is to be suppressed for FM order. The electronic and nuclear molecular fields (MF) are given by

$$\begin{aligned} h_e^\lambda &= h + \sigma m_s I_e \langle S_x \rangle_{\bar{\lambda}} - A \langle I_z \rangle_\lambda \\ h_n^\lambda &= m_s A \langle S_x \rangle_\lambda \end{aligned} \quad (5)$$

Here $\sigma = \pm 1$ for FM and AFM, respectively, and $I_e = z|I_0|$ is the effective exchange with $z = \text{N.N.}$ coordination number. We note that the nuclear Zeeman term in Eq. (3) which would give a direct contribution $g_n \mu_n H$ to h_n^λ above is neglected [28], assuming $g_n \mu_n H \ll m_s A \langle S_x \rangle_\lambda$ in the present context. Because the hyperfine term does not mix nuclear spin states in this Ising type model the Hamiltonian will factorise for each $\tau = I_z$ subspace ($|\tau| \leq I$) and then we obtain

$$\hat{h}_{mf}^{\lambda\tau} = \frac{\Delta}{2} \begin{pmatrix} 1 + 2\tau\gamma'_{n\lambda} & -\gamma'_{e\lambda} \\ -\gamma'_{e\lambda} & -1 + 2\tau\gamma'_{n\lambda} \end{pmatrix}, \quad (6)$$

where we defined the dimensionless MF's $\gamma'_{e\lambda} = m_s h_e^\lambda / \Delta \equiv: \hat{\Delta}_{e\lambda}$ and $\gamma'_{n\lambda} = h_n^\lambda / \Delta \equiv: \hat{\Delta}_{n\lambda}$. This may readily be diagonalised leading to the coupled electronic-nuclear MF energy levels given by

$$E_{\lambda s}^\tau = \frac{\Delta}{2} [s(1 + \gamma'^2_{e\lambda})^{\frac{1}{2}} + 2\tau\gamma'_{n\lambda}] \quad (7)$$

where $s = \pm 1$ refers to the two MF shifted singlet states originating from original $|1\rangle, |0\rangle$ states, respectively. The second term describes the splitting of nuclear spin states by the MF. Due to the Ising -type model the eigenstates are still product states of electronic and nuclear states and therefore the transformation to them simply factorises as described by

$$\begin{aligned} |E_{\lambda+}^\tau\rangle &= \cos(\theta_\lambda) |1\tau\rangle - \sin(\theta_\lambda) |0\tau\rangle \\ |E_{\lambda-}^\tau\rangle &= \sin(\theta_\lambda) |1\tau\rangle + \cos(\theta_\lambda) |0\tau\rangle \end{aligned} \quad (8)$$

with the mixing angle given by $\tan 2\theta_\lambda = \gamma'_{e\lambda}$. The spectrum which is illustrated as an inset in Fig. 1 is highly symmetric which facilitates further analytical treatment. In the basis of MF eigenstates the two-singlet pseudo spin is represented by

$$\begin{aligned} S'_x &= \frac{1}{2} \begin{pmatrix} -\sin 2\theta_\lambda & \cos 2\theta_\lambda \\ \cos 2\theta_\lambda & \sin 2\theta_\lambda \end{pmatrix} \\ &= \frac{1}{2}(1 + \gamma'^2_{e\lambda})^{\frac{1}{2}} \begin{pmatrix} -\gamma'_{e\lambda} & 1 \\ 1 & \gamma'_{e\lambda} \end{pmatrix} \end{aligned} \quad (9)$$

Since the nuclear spin states are not mixed by the Ising-like hyperfine term nuclear spin operator I_z is unchanged.

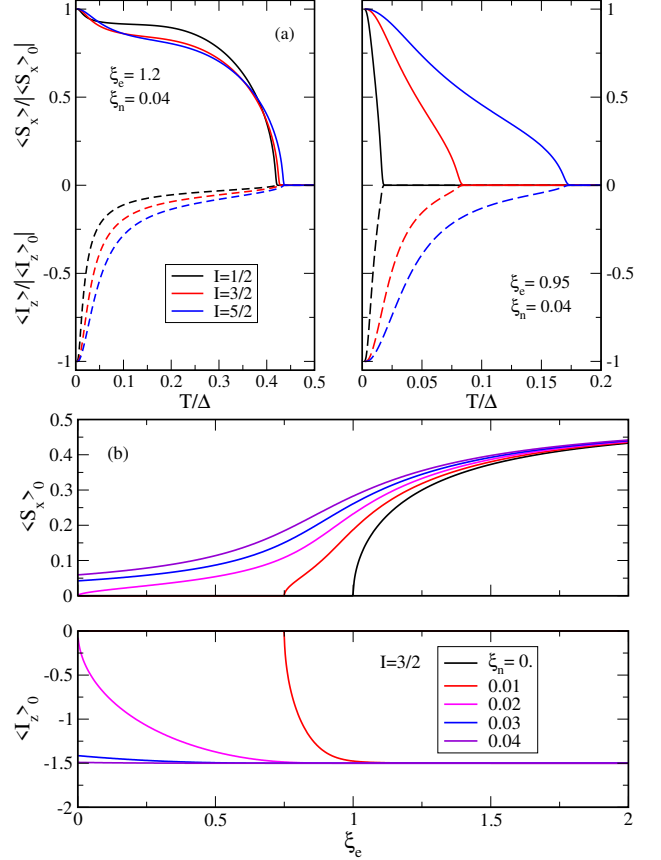


FIG. 2. (a) Dependence of (normalized) electronic and nuclear order parameters on temperature for hyperfine coupling $\xi_n = 0.04$. Left panel: For a value of ξ_e above the QCP $\xi_e^c = 1$ (without hyperfine coupling), shown for various nuclear spin size. The small differences in T_m for the three cases corresponds to Fig. 1 in the region above the QCP. Right panel: For a value of ξ_e below the QCP where order is established only due to the finite hyperfine coupling control parameter ξ_n . Here the electronic and nuclear order parameters exhibit similar T - dependence in contrast to (a) but T_m now depends strongly on the size of the nuclear spin I . (b) Electronic and nuclear saturation moments ($T/\Delta = 0.001$) as function of control parameters. When $T < T_m(\xi_e, \xi_n)$ (Fig. 1) $\langle S_x \rangle_0$ is finite and $\langle I_z \rangle \approx -I$. Otherwise both drop to zero.

III. THE CRITICAL TEMPERATURE FOR INDUCED ORDER OF ELECTRONIC AND NUCLEAR MOMENTS

Before solving the MF selfconsistency equations for the order parameters we can determine the phase boundary, i.e. the critical temperature $T_m(\xi_e, \xi_n, I)$ as function of control parameters ξ_e, ξ_n introduced below and nuclear spin size I by starting from the paramagnetic regime. It is obtained from the divergence of the static RPA susceptibility at the critical temperature for the zone center or zone boundary wave vectors of the FM or AFM structure, respectively. The static single ion susceptibility for a multilevel system corresponding to opera-

tor $O = J_z (= m_s S_x)$, I_z is generally given by

$$\begin{aligned} \chi_0^O(T, h') &= \sum_{E_\mu \neq E_{\mu'}} |\langle \mu | O | \mu' \rangle|^2 \frac{p_\mu - p_{\mu'}}{E_{\mu'} - E_\mu} \\ &+ \frac{1}{T} \left[\sum_{E_\mu = E_{\mu'}} |\langle \mu | O | \mu' \rangle|^2 p_\mu - \langle O \rangle^2 \right], \quad (10) \end{aligned}$$

where $|\mu\rangle = |s\rangle \otimes |\tau\rangle$ are the paramagnetic states with $s = 0, 1$ denoting the singlets and $\tau = -I..I$ the nuclear spin states and E_μ, p_μ their energies and thermal populations, respectively. There is no mixing or splitting of these states in the paramagnetic regime and then simply the susceptibilities are decoupled with

$$\chi_0^J = \frac{m_s^2}{2\Delta} \tanh \frac{\Delta}{2T}; \quad \chi_0^I = \frac{\frac{1}{3}I(I+1)}{T} \quad (11)$$

The q -dependent RPA susceptibility corresponding to the Hamiltonian in Eq. (3) is then obtained for both operators as

$$\chi_{\mathbf{q}}^{J,I} = \frac{\chi_0^{J,I}}{1 - \chi_0^J(I_{\mathbf{q}} + A^2 \chi_0^I)} \quad (12)$$

which includes the effect of the hyperfine coupling proportional to A . Here $I_q = zI_0\gamma_q$ ($I_e = z|I_0|$) is the intersite-exchange Fourier transform with $\gamma_q = z^{-1}\sum_{\delta} \exp(iq \cdot \delta)$ where z is the coordination number and δ designates the N.N. positions. The transition temperature to the induced magnetic order is then given by the condition of vanishing denominator in Eq. (12). This leads finally to the implicit equation for $T_m(\xi_e, \xi_n, I)$:

$$\left[\xi_e + \frac{1}{3} I(I+1)(2\xi_n)^2 \frac{\Delta}{2T_m} \right] \tanh\left(\frac{\Delta}{2T_m}\right) = 1 \quad (13)$$

Here we introduced the dimensionless electronic and nuclear control parameters

$$\xi_e = \frac{m_s^2 I_e}{2\Delta}; \quad \xi_n = \frac{m_s A}{2\Delta} \quad (14)$$

which characterise intersite exchange and hyperfine coupling strength, respectively. For vanishing hyperfine coupling ($\xi_n = 0$) one obtains explicitly the purely electronic induced moment transition temperature

$$T_m^0(\xi_e) = \frac{\Delta}{2 \tanh^{-1}\left(\frac{1}{\xi_e}\right)} \quad (15)$$

This is shown in Fig. 1 (black line) together with the general numerical solution of Eq.(13) for nonzero hyperfine coupling and it will be further discussed in Sec. VII. Importantly the QCP at $\xi_e = 1$ for vanishing hyperfine control parameter ξ_n is now replaced by a crossover for finite ξ_n from a high T_m CEF induced moment region where $T_m \approx T_m^0$ to a low $T_m \ll \Delta$ nuclear moment dominated ordering region (see also Fig. 11). For $\xi_e \rightarrow 0$ we have the asymptotic form derived from Eq. (13):

$$T_m \simeq \frac{2}{3} \Delta I (I+1) \xi_n^2 (1 - \xi_e)^{-1} \quad (16)$$

which approaches a constant independent of ξ_e in this limit.

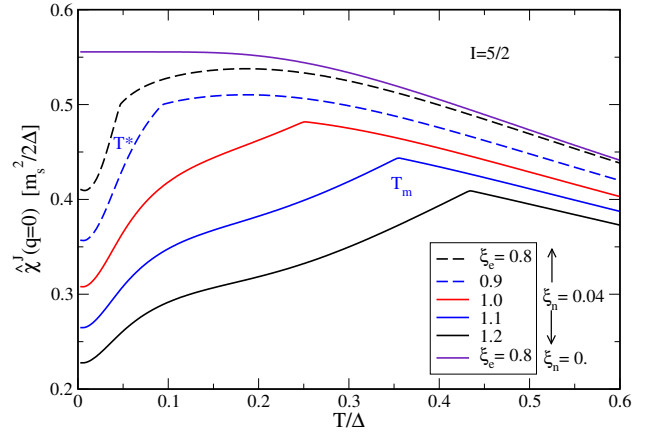


FIG. 3. Homogeneous electronic RPA susceptibility $\chi^J(\mathbf{q}=0)$ (Eqs. (12,27)) in paramagnetic and AFM ordered regimes for control parameter ξ_e above (> 1) and below (< 1) critical value. For the former a clear cusp at the induced magnetic order occurs. For subcritical values the cusp at T_m is much diminished but a clear low temperature depression at $T^* \approx \xi_n \Delta$ corresponding to nuclear splitting energies remains. The upper curve is the reference for $\xi_n = 0$ for the paramagnetic CEF vanVleck susceptibility.

IV. SELFCONSISTENCY EQUATIONS FOR ELECTRONIC AND NUCLEAR MOMENTS

From the derivations in Sec. II we can now obtain the self-consistent MF equations for electronic and nuclear moments as

$$\begin{aligned}\langle S_x \rangle_\lambda &= \frac{1}{2} \frac{1}{\hat{\Delta}_e} [m_s h' + 2(\sigma \xi_e \langle S_x \rangle_{\bar{\lambda}} - \xi_n \langle I_z \rangle_\lambda)] \hat{P}_{e\lambda}(T) \\ \langle I_z \rangle_\lambda &= -\frac{1}{2} \hat{P}_{n\lambda}(T; \langle S_x \rangle_\lambda) \end{aligned} \quad (17)$$

with $\hat{P}_{(e,n)\lambda}$ defined below (Eq. (22)). Using Eq. (5) the corresponding molecular fields, normalised to Δ , may be expressed as

$$\begin{aligned}\gamma'_{e\lambda} &= m_s h' + 2(\sigma \xi_e \langle S_x \rangle_{\bar{\lambda}} - \xi_n \langle I_z \rangle_{\lambda}) \\ \gamma'_{n\lambda} &= 2\xi_n \langle S_x \rangle_{\lambda}\end{aligned}\quad (18)$$

where $h' = h/\Delta$ is the dimensionless field strength. With these expressions the MF singlet splitting and nuclear spin splittings are given by

$$\hat{\Delta}_{e\lambda} = (1 + \gamma_{e\lambda}^2)^{\frac{1}{2}}; \quad \hat{\Delta}_{n\lambda} = 2\xi_n \langle S_x \rangle_\lambda = \gamma_{n\lambda}' \quad (19)$$

respectively, which are again normalised according to $\hat{\Delta}_{e\lambda} = \Delta_{e\lambda}/\Delta$ and $\hat{\Delta}_{n\lambda} = \Delta_{n\lambda}/\Delta$. The former is always positive while the latter, which is caused by the hyperfine coupling to the induced moment, may have both signs depending on the sublattice. This allows us also to present the $2 \times (2I+1)$ split energy levels at each sublattice $\lambda = A, B$ in the compact form

$$E_{\lambda s}^{\tau} = \frac{\Delta}{2} (s \hat{\Delta}_{e\lambda} + 2\tau \hat{\Delta}_{n\lambda}) \quad (20)$$

TABLE I. Magnetic characteristic quantities of 4f shell for non-Kramers rare earth elements with J denoting ground state total angular momentum, g_J the associated Landé factor and $\mu_{eff} = g_J \sqrt{J(J+1)}$ the effective moment. These stable rare earth isotopes have 100% abundance ratio with resulting unique nuclear ground state spin I and nuclear moment μ (with $\mu_n = e\hbar/2M_p c$ defining the nuclear magneton; M_p =proton mass) and hyperfine coupling constant A .

RE ³⁺ ion	¹⁴¹ Pr	¹⁵⁹ Tb	¹⁶⁹ Tm
J	4	6	6
g_J	$\frac{4}{5}$	$\frac{3}{2}$	$\frac{7}{6}$
$\mu_{eff} [\mu_B]$	3.58	9.72	7.56
I	$\frac{5}{2}$	$\frac{3}{2}$	$\frac{1}{2}$
$\mu [\mu_n]$	3.92	1.52	-0.20
A [mK]	52.5[7]	71.9[29]	-18[30]

where the electronic two-singlet and the nuclear indices are $s = \pm, \tau = -I..I$, respectively. The thermal occupations of individual levels are given by $p_{\lambda s}^{\tau} = Z_{\lambda}^{-1} \exp(-E_{\lambda s}^{\tau})$ where Z_{λ} is the partition function for sublattice $\lambda = A, B$. Because the Ising type hyperfine interaction does not mix the products of electronic and nuclear states the partition function factorises according to $Z_{\lambda} = Z_{e\lambda} \cdot Z_{n\lambda}$ and the factors are given by

$$Z_{e\lambda} = 2 \cosh \left[\left(\frac{\Delta}{2T} \right) \hat{\Delta}_{e\lambda} \right]$$

$$Z_{n\lambda} = 2 \sum_{\tau=\frac{1}{2}}^I \cosh \left[\left(\frac{\Delta}{2T} \right) 2\tau \hat{\Delta}_{n\lambda} \right] \quad (21)$$

The form of $Z_{n\lambda}$ is valid for *noninteger* nuclear spin $I = \frac{1}{2}, \frac{3}{2}, \dots$ which is the case for the isotopes of 4f elements which we have in mind here (Table I). Then the differences of thermal populations appearing in Eq. (17) may be derived as

$$\hat{P}_{e\lambda}(T) = \tanh \frac{\Delta}{2T} \hat{\Delta}_{e\lambda}$$

$$\hat{P}_{n\lambda}(T) = 4Z_{n\lambda}^{-1} \sum_{\tau=\frac{1}{2}}^I \tau \sinh \left[\left(\frac{\Delta}{2T} \right) 2\tau \hat{\Delta}_{n\lambda} \right] \quad (22)$$

These population functions depend implicitly on the induced moments $\langle S_x \rangle_{\lambda}$ and $\langle I_z \rangle_{\lambda}$ for each sublattice via the excitation energies $\hat{\Delta}_{e\lambda}, \hat{\Delta}_{n\lambda}$ which have a sublattice λ - dependent size for finite field h . In zero field the sublattice dependence reduces to just a sign difference given by $P_{n\lambda}(T) = sign(\lambda)P_{\lambda}(T)$ with $sign(\lambda) = \pm 1$ for $\lambda = A, B$. The coupled MF Eqs. (17) for $\langle S_x \rangle$ and $\langle I_z \rangle$ have to be solved numerically for each nuclear spin size I as a function of control parameters ξ_e and ξ_n characterising the intersite electronic exchange and the on-site hyperfine coupling. For the special case with nuclear spin $I = \frac{1}{2}$ we may write the selfconsis-

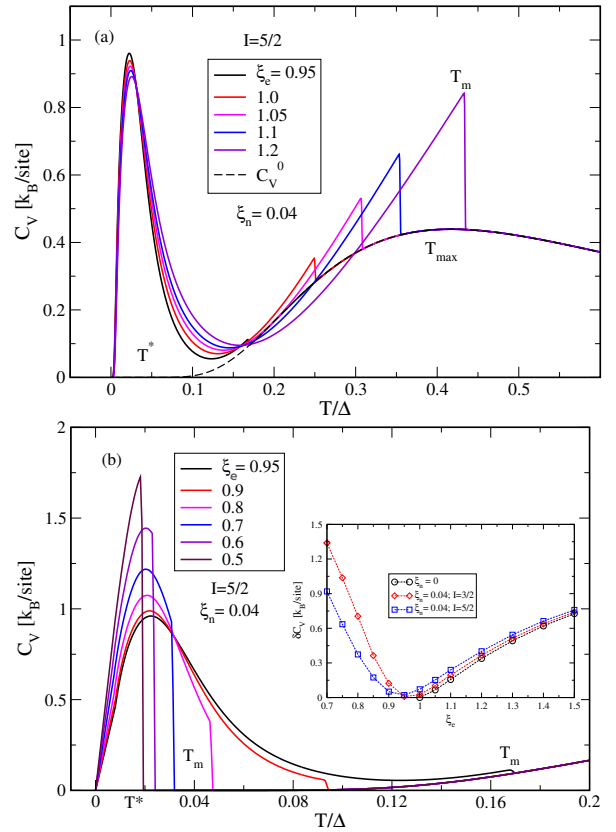


FIG. 4. (a) Specific heat of the hyperfine-coupled singlet-singlet CEF and nuclear spin $I = \frac{3}{2}$ for various sub- and above critical electronic control parameters ξ_e . The typical three-peak appearance is displayed: i) the broad underlying CEF Schottky peak (dashed line) at T_{max} due to the CEF splitting, ii) for $\xi_e > 1$ a superposed induced ordering peak at T_m and iii) a low temperature nuclear specific heat peak with maximum at $T^* \simeq \xi_n \Delta$ due to the nuclear spin splitting caused by the order at T_m . (b) For subcritical ξ_e but finite ξ_n the ordering at T_m shows crossover into the region dominated by the hyperfine coupling around T^* (see Fig. 1). Inset shows evolution of specific heat jump $\delta C_V(T_m)$ with nonmonotonic change from induced moment regime $\xi_e > 1$ (corresponding to (a)) to hyperfine dominated regime $\xi_e < 1$ (associated with (b)).

tency equations in Eq. (17) more explicitly as

$$\langle S_x \rangle_{\lambda} = \frac{1}{2} \frac{1}{\hat{\Delta}_{e\lambda}} \left\{ m_s h' - 2\xi_e \langle S_x \rangle_{\bar{\lambda}} + \xi_n \tanh \left[\left(\frac{\Delta}{2T} \right) (2\xi_n \langle S_x \rangle_{\lambda}) \right] \right\} \times \tanh \left[\left(\frac{\Delta}{2T} \right) \hat{\Delta}_{e\lambda} \right]$$

$$\hat{\Delta}_{e\lambda} = \left\{ 1 + \left(m_s h' - 2\xi_e \langle S_x \rangle_{\bar{\lambda}} + \xi_n \tanh \left[\left(\frac{\Delta}{2T} \right) (2\xi_n \langle S_x \rangle_{\lambda}) \right] \right)^2 \right\}^{\frac{1}{2}}$$

$$\langle I_z \rangle_{\lambda} = -\frac{1}{2} \tanh \left[\left(\frac{\Delta}{2T} \right) (2\xi_n \langle S_x \rangle_{\lambda}) \right] \quad (23)$$

Examples for the temperature and field evolution of electronic and nuclear order parameters are shown in Figs 2,9. For the FM the phase transition turns into a continuous crossover at T_m while in the AFM it persists up to a critical field. The critical field curve $h_{cr}(T)$ is implicitly defined by the vanishing of the staggered moment $M_s = \frac{1}{2}(\langle S_x \rangle_A - \langle S_x \rangle_B)$ via

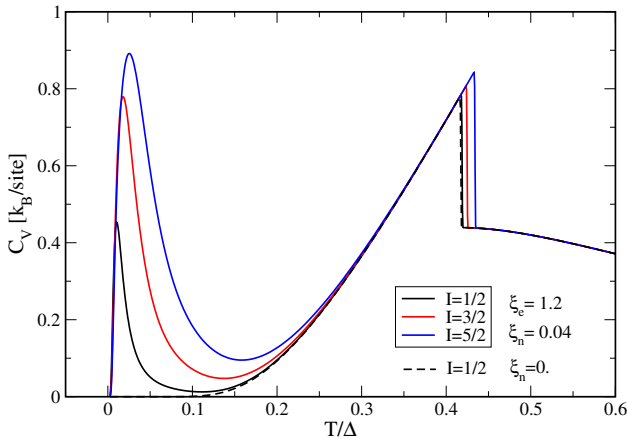


FIG. 5. Specific heat curves for fixed control parameters ξ_e, ξ_n and various nuclear spin size I which strongly influences the peak height due to entropy $\sim \ln(2I + 1)$ contained in it. The dashed line corresponds to the CEF specific heat for $\xi_n = 0$ (Eq. (32)).

the equation $M_s(h_{cr}, T) = 0$ and likewise this determines the field dependence of $T_m(h)$. The phase boundary is strongly influenced by the action of the hyperfine coupling as shown in Fig. 8 and its resulting anomalous characteristics will be discussed further in Sec. VII.

A. Susceptibility in the ordered regime

The electronic and nuclear single site zero-field ($h=0$) susceptibilities in the ordered phase may also be derived using the transformed pseudo spin operator of Eq. (9) and the expression in Eq. (10). We obtain for the electronic part $\chi_0^J(T) = (\frac{m_s^2}{2\Delta})\hat{\chi}_0^J(T)$ where the dimensionless quantity is

$$\hat{\chi}_0^J(T) = \frac{1}{\hat{\Delta}_e^3} \tanh \frac{\Delta_e}{2T} + (1 - \frac{1}{\hat{\Delta}_e^2}) \left(\frac{\Delta}{2T} \right) \cosh^{-2} \frac{\Delta_e}{2T} \quad (24)$$

which now contains a modified vanVleck and a pseudo-Curie term. Note that the latter vanishes for small temperature despite the $(1/T)$ factor due to the other exponential population factor. In the paramagnetic phase $\Delta_e = \Delta$ and then the expression in Eq. (11) is recovered. The nuclear spin susceptibility is now modified due to the splitting of nuclear spin states and leads to another pseudo-Curie expression $\chi_0^I(T) = (\frac{2}{\Delta})\hat{\chi}_0^I(T)$ and likewise

$$\hat{\chi}_0^I(T) = \left(\frac{\Delta}{2T} \right) [\hat{P}_n^C(T) - \langle I_z \rangle^2] \quad (25)$$

with an additional nuclear level population function defined by

$$\hat{P}_n^C(T) = 2Z_n^{-1} \sum_{\tau=\frac{1}{2}}^I \tau^2 \cosh \left[\left(\frac{\Delta}{2T} \right) 2\tau \hat{\Delta}_n \right] \quad (26)$$

On approaching $T=0$ the two terms in Eq. (25) approach I^2 and compensate leading to exponential suppression of the

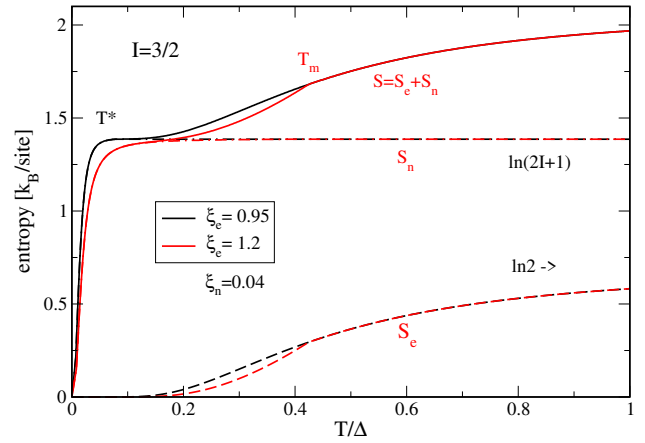


FIG. 6. Electronic (S_e), nuclear (S_n) and total entropy S as function of temperature for two above (red) and below (black) critical control parameters. The entropy release for S_e is mostly due to depopulation of singlets but also due to induced ordering at T_m . The nuclear entropy is released due to the $(2I + 1)$ nuclear level splitting caused by appearance of $\langle S_x \rangle$ at T_m . For subcritical $\xi_n = 0.95$ the nuclear entropy is directly released by the nuclear dominated order around $T_m \approx T^*$ (cf. Figs. 1,4(b)).

Curie prefactor $(1/T)$. In the paramagnetic state with $\langle I_z \rangle = 0$ and $\hat{P}_n^C = \frac{1}{3}I(I+1)$ this reduces to Eq. (11).

Using the above results the homogeneous electronic RPA susceptibility in the AF case, for paramagnetic and ordered regime may finally be expressed according to Eq. (12) as

$$\chi^J(\mathbf{q} = 0) = \frac{\left(\frac{m_s^2}{2\Delta} \right) \hat{\chi}_0^J(T)}{1 + [\xi_e + (2\xi_n)^2 \hat{\chi}_0^I(T)] \hat{\chi}_0^J(T)} \quad (27)$$

The physical electronic susceptibility then has to be multiplied by $(g_J \mu_B)^2$. A similar nuclear RPA susceptibility is obtained by replacing the numerator in the above equation with $(2/\Delta)\hat{\chi}_0^I$. The latter has a physical prefactor $(g_n \mu_n)^2$. Since the nuclear magneton $\mu_n \ll \mu_B$ it gives negligible contribution to the susceptibility. The temperature dependence of the homogeneous susceptibility in Eq. (27) is shown in Fig. 3 and discussed in Sec. VII.

V. ELECTRONIC AND NUCLEAR PARTS OF THE SPECIFIC HEAT, ENTROPY AND INTERNAL ENERGY

Of major interest is the signature of the electronic and nuclear contributions to the specific heat since caloric experiments are most common in the low temperature regime in question. We approach this problem by first calculating the thermodynamic potentials like entropy $S(T)$ and internal energy $U(T)$. The entropy per sublattice site is given in terms of level occupation probabilities $p_{s\tau}(T)$ as

$$S_\lambda(T) = - \sum_{s\tau} p_{s\tau} \ln p_{s\tau} \quad (28)$$

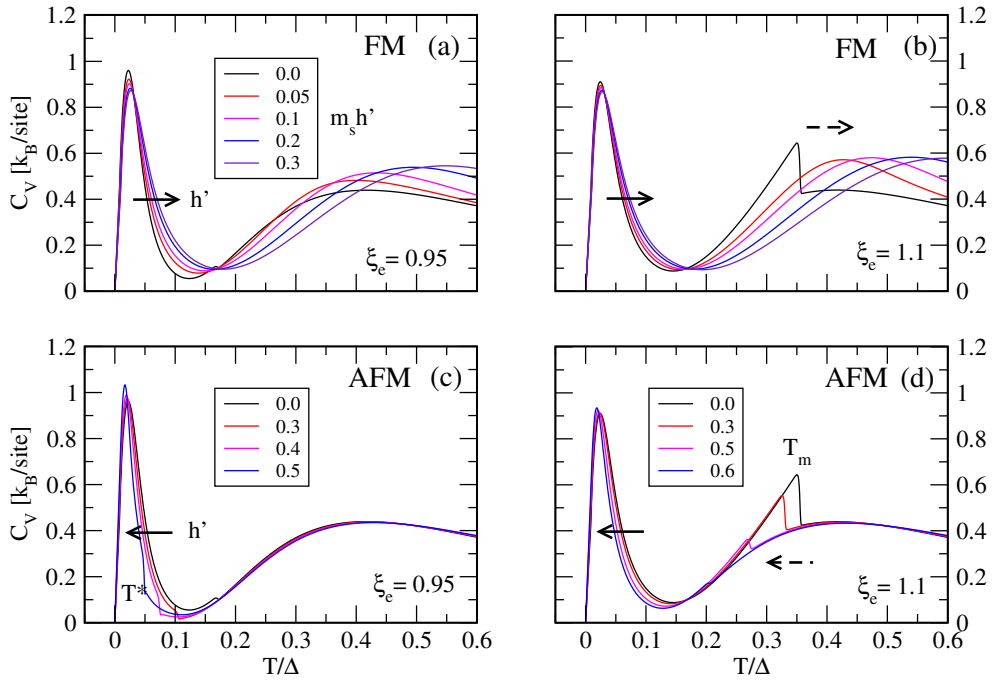


FIG. 7. Nuclear ($I = \frac{5}{2}$) and electronic specific heat evolution in external field for FM (a,b) and AFM(c,d) cases for sub- and above- critical control parameter ξ_e and $\xi_n = 0.04$ throughout. Dimensionless field strength $m_{sh'}$ is given in the boxes (equivalent for a,b). Evolution of anomalies with *increasing* h' is indicated by arrows. In the FM case larger fields lead to a broadening of the nuclear peak (a,b) at $T^*/\Delta \simeq \xi_n$ (a,b) and a rapid suppression, broadening and shift to higher temperature of the zero field jump at T_m (b). In contrast for the AFM case the nuclear peak narrows with increasing field (c,d) while the AFM transition jump at T_m (d) prevails but is diminished and shifted to lower temperature.

which may be separated into an electronic and nuclear part $S_\lambda = S_{e\lambda} + S_{n\lambda}$ according to

$$S_{e\lambda} = -\frac{\Delta}{2T} \hat{\Delta}_{e\lambda} \hat{P}_{e\lambda}(T) + \ln\{2 \cosh\left[\left(\frac{\Delta}{2T}\right) \hat{\Delta}_{e\lambda}\right]\} \quad (29)$$

$$S_{n\lambda} = -\frac{\Delta}{2T} \hat{\Delta}_{n\lambda} \hat{P}_{n\lambda}(T) + \ln\{2 \sum_{\tau=\frac{1}{2}}^I \cosh\left[\left(\frac{\Delta}{2T}\right) 2\tau \hat{\Delta}_{n\lambda}\right]\}$$

Note that this expression is invariant against a constant shift of the combined level scheme. The internal energy which is related by $U_\lambda(T) = TS_\lambda(T) - T \ln Z_\lambda$ is obtained as

$$U_\lambda(T) = -\frac{\Delta}{2} \hat{\Delta}_{e\lambda} \hat{P}_{e\lambda}(T) + \Delta \sigma \xi_e \langle S_x \rangle_\lambda \langle S_x \rangle_{\bar{\lambda}} \quad (30)$$

Formally the nuclear part has a similar structure. But in this case the first term due to the nuclear spin splitting is exactly compensated by the second constant MF term describing the hyperfine interaction with the electronic moment. However, the nuclear degrees are implicitly incorporated in the electronic splitting $\hat{\Delta}_{e\lambda}(T)$ and $\langle S_x \rangle_\lambda$. The total entropies and internal energies (per lattice site) are then obtained by averaging over the sublattices A,B in the AFM ($\sigma = -1$) case, while the sublattice index λ may be ignored in the FM case ($\sigma = 1$). Then the specific heat is obtained from the thermodynamical potentials via

$$C_V(T) = \left(\frac{\partial U}{\partial T}\right)_V = T \left(\frac{\partial S}{\partial T}\right)_V \quad (31)$$

by numerical differentiation which has been checked to lead to identical results for both expressions. In the case of zero hyperfine coupling $\xi_n = 0$ only the electronic singlet degrees contribute and then the specific heat may be derived in closed form from the above equations as [3].

$$\begin{cases} C_V(T) = \left(\frac{\Delta_T}{2T}\right)^2 \left(\cosh^2 \frac{\Delta_T}{2T} - \frac{\Delta_0}{2T}\right)^{-1} & T \leq T_m \\ C_V^0(T) = \left(\frac{\Delta}{2T}\right)^2 \cosh^{-2} \frac{\Delta}{2T} & T > T_m \end{cases} \quad (32)$$

for magnetic and paramagnetic phases, respectively, where we used the abbreviation $\Delta_T = \Delta \hat{\Delta}_e(T)$. $C_V^0(T)$ is the paramagnetic background Schottky anomaly which peaks around $T_{max} = 0.42\Delta$ for the two-singlet system. It is shown as a reference by the dashed line in Fig.4(a). $C_V(T)$ exhibits the jump at the induced moment transition temperature T_m^0 . Expressions of the jump size at T_m^0 as function of control parameter ξ_e are given in Ref. 3. It tends to zero when approaching the QCP from above, i.e. $\xi_e \rightarrow 1 + \delta$; $\delta \ll 1$. The field and temperature dependence of the specific heat in the above general expressions for finite ξ_n in Eqs. (30,30,31) is contained in the excitation energies $\Delta_{e,n}^\lambda$ and the order parameters $\langle S_x \rangle_\lambda$, $\langle I_z \rangle_\lambda$ obtained from the selfconsistent solution of MF equations Eq (17). The (magneto-) caloric properties of the model are presented in Figs. 4,5 and 7 and are discussed in Sec. VII.

VI. INFLUENCE OF NUCLEAR ELECTRIC QUADRUPOLE SPLITTING

In the previous analysis we have assumed that the nuclear spin states are $(2I + 1)$ -fold degenerate. However for $I \geq \frac{3}{2}$ an electric field gradient (EFG) at the nuclear site originating from the occupied electronic states and resulting in a quadrupolar potential will lift the degeneracy into pairs of time reversed states with $I_z = \pm\tau$. It is then to be expected to influence significantly the magnetic transition temperature, in particular around and below the QCP at $\xi_e = 1$ where the hyperfine interaction plays an important role. The change in transition temperature due to the nuclear quadrupole splitting will now be investigated.

The quadrupolar Hamiltonian for nuclear spins is given by [31]

$$H_Q^n = \frac{\zeta}{4I(I-1)} \sum_i [3I_z^2(i) - I(I+1)] \quad (33)$$

with the quadrupolar coupling constant $\zeta = \frac{e^2 q Q}{\hbar}$ where Q is the nuclear quadrupole moment and $eq = V_{zz}$ the uniaxial EFG. This causes a splitting of nuclear spin states already in the paramagnetic phase which is added to the splitting caused by the molecular field in the induced moment phase. Together this leads to multiplet energy levels given by an extension of Eq. (7) as

$$E_{\lambda s}^{\tau} = \frac{\Delta}{2} [s\hat{\Delta}_{e\lambda} + 2\tau\hat{\Delta}_{n\lambda} + \tau^2\hat{\Delta}_Q] \quad (34)$$

where the last term describes the paramagnetic quadrupolar splitting with $\hat{\Delta}_Q = \Delta_Q/\Delta = 3\zeta/[2I(I-1)\Delta]$ which can have both signs depending on the signs of the EFG, the nuclear quadrupole moment and on I . A constant shift which has no influence on the thermodynamics has been omitted. The splitting will modify the nuclear spin susceptibility. For this purpose we need to obtain the population factors of the split nuclear levels. They are now given by

$$\begin{aligned} p_{\lambda}^{\tau} &= Z_n^{-1} \exp\left[-\frac{\Delta}{2T}(2\tau\lambda\hat{\Delta}_n + \tau^2\hat{\Delta}_Q)\right] \\ Z_n &= 2 \sum_{\tau=1/2}^I \exp\left(-\frac{\Delta}{2T}\tau^2\hat{\Delta}_Q\right) \cosh \frac{\Delta}{2T} 2\tau\hat{\Delta}_n \end{aligned} \quad (35)$$

The electronic level occupations and partition functions and therefore the susceptibility $\chi_0^J(T)$ are unchanged because the eigenstates are not modified by the Hamiltonian of Eq. (33). With the above results we can then obtain the quadrupolar modified nuclear spin susceptibility as

$$\begin{aligned} \chi_0^I &= \frac{\hat{P}_n^Q(T)}{T} \\ \hat{P}_n^Q(T) &= 2Z_n^{-1} \sum_{\tau=1/2}^I \tau^2 \exp\left(-\frac{\Delta}{2T}\tau^2\hat{\Delta}_Q\right) \end{aligned} \quad (36)$$

It is still of the Curie type due to splitting into nuclear spin doublets, however, the numerator is no longer a Curie constant

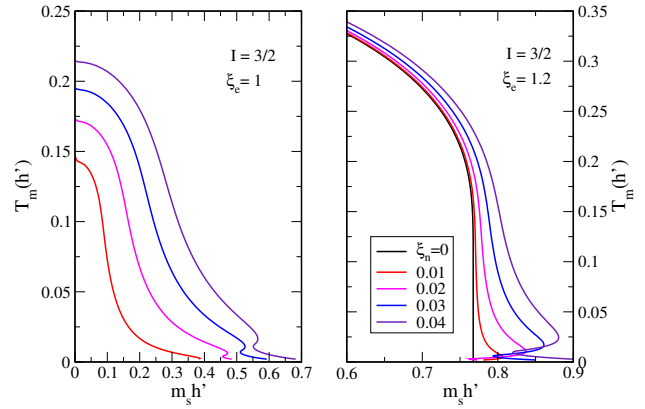


FIG. 8. Field dependence of the AFM transition temperature in the QCP regime (left) and the exchange dominated regime (right) for various hyperfine coupling strengths ξ_n . In the left panel T_m increases rapidly with ξ_n and starts to develop reentrant behaviour for large critical fields (low $T_m(h')$). This is even more pronounced in the right panel ($\xi_e > 1$) for increasing ξ_n , cf. Figs. 9,10.

as in Eq. (11) but a temperature dependent occupation function. It is interesting to consider three limiting cases valid for any $I \geq \frac{3}{2}$: i) For $T \gg |\Delta_Q|$ we have $\hat{P}_n^Q(T) \rightarrow \frac{1}{3}I(I+1)$ ii) for $T \ll |\Delta_Q|$ and $\Delta_Q > 0$ we obtain with $I_{eff} := \frac{1}{2}$ $\hat{P}_n^Q(T) \rightarrow \frac{1}{3}I_{eff}(I_{eff}+1) = \frac{1}{4} < \frac{1}{3}I(I+1)$. iii) finally for $T \ll |\Delta_Q|$ and $\Delta_Q < 0$ we get $\hat{P}_n^Q(T) \rightarrow I^2 > \frac{1}{3}I(I+1)$. This means that depending on the sign of the quadrupolar splitting and its size as compared to the transition temperature the effective Curie numerator may be smaller or larger than the numerator $\frac{1}{3}I(I+1)$ for the degenerate nuclear spin states. Therefore a finite Δ_Q may lead to a decrease or increase in the nuclear ordering temperature for positive or negative sign, respectively.

Inserting χ_0^I from Eq. (36) and the previous, unchanged χ_0^J from Eq. (11) into the paramagnetic RPA susceptibility of Eq. (12) the condition for the divergence of the latter leads now to a generalized implicit equation for the transition temperature $T_m(\xi_e, \xi_n, \hat{\Delta}_Q, I)$ that contains the effect of the quadrupolar splitting. It is given by

$$[\xi_e + \hat{P}_n^Q(T_m)(2\xi_n)^2 \frac{\Delta}{2T_m}] \tanh\left(\frac{\Delta}{2T_m}\right) = 1 \quad (37)$$

which may be obtained from the previous degenerate nuclear case given in Eq. (13) simply by replacing the Curie constant $\frac{1}{3}I(I+1)$ by the effective temperature dependent Curie numerator in Eq. (36). From this it is clear that the quadrupolar interaction dependence of $T_m(\hat{\Delta}_Q)$ is limited by the curves for actual nuclear spin size I and quadrupolar ground state doublet with $\tau = \pm\frac{1}{2}$ or $\tau = \pm I$. This is shown in Figs. 11,12 and discussed in Sec. VII.

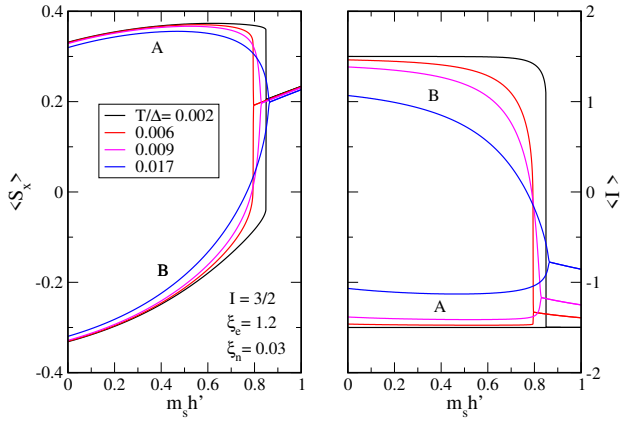


FIG. 9. Field dependence of electronic $\langle S_x \rangle$ and nuclear $\langle I_z \rangle$ order parameters on A,B sublattices (left and right panels) in the low temperature reentrant regime of the right panel in Fig. 9. At the lowest temperature the transition appears is first order like while it changes to clear second order appearance when moving from the sharp minimum of the critical field to its maximum in Fig. 8. The critical field h' varies nonmonotonic with temperature.

VII. DISCUSSION OF NUMERICAL RESULTS AND MATERIAL EXAMPLES

The main focus of the previous analysis is firstly the dependence of the transition temperature or phase diagram of induced moment magnetism on the electronic and nuclear control parameters, in particular the removal of the induced moment QCP by the hyperfine coupling. Secondly the interplay and competition of various mechanisms on the entropy release witnessed by the specific heat anomalies, namely, CEF level depopulation, exchange dominated induced moment order and hyperfine dominated nuclear ordering. And thirdly the hyperfine coupling leads to anomalous nonmonotonic critical field dependence on temperature or equivalently a reentrance signature of magnetic order for large fields. The numerical results of these important effects of coupled CEF and nuclear degrees of freedom will now be discussed in detail for typical cases.

First we have to remark on the parameter regions which are realistic. The electronic control parameter ξ_e will be considered in the region of true induced moment order above the QCP $\xi_e = 1$ but not too large and for subcritical region $\xi_e < 1$ where the hyperfine interaction plays an important role. The nuclear control parameter $\xi_n = m_s A / 2\Delta$ sets the hyperfine coupling in relation to the two-singlet CEF splitting. We take the CEF model in Eq.(1) with equal admixture coefficients corresponding to $\alpha = \pi/2$ which leads to the total angular momentum matrix element $m_s = 8$. We assume a rather small singlet splitting of $\Delta = 5\text{K}$ in order to present the electronic and nuclear specific heat anomalies in graphs with linear rather than a distorted logarithmic temperature scale. This is not a restrictive assumption from the theory but just convenient for the presentation. Using the typical size of $A \approx 50\text{ mK}$ given in Table I for the potential singlet

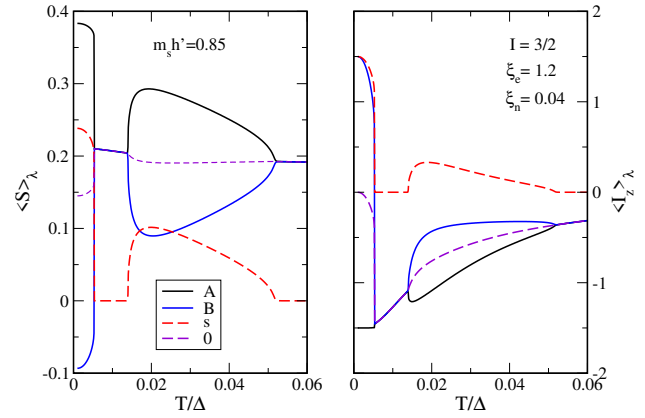


FIG. 10. Complementary reentrant magnetic order caused by finite hyperfine coupling as function of temperature for large field $m_s h' = 0.85$ close to the maximum critical field in Fig. 8(b). Here the order parameter is the staggered (red dashed) $M_s = \frac{1}{2}(\langle S_x \rangle_A - \langle S_x \rangle_B)$ and $M_0 = \frac{1}{2}(\langle S_x \rangle_A + \langle S_x \rangle_B)$ the homogeneous (violet dashed) electronic polarisation (left panel) and likewise for the nuclear spin degrees of freedom (right panel). Note there is an intermediate temperature regime where the staggered order parameters reemerge.

ground state candidate ions the nuclear control parameter is of the order $\xi_n \approx 0.04 \ll 1$. The sign of ξ_e or ξ_n has no influence because the spectra in Eqs. (20,34) are invariant under $\xi_n, \tau \rightarrow -\xi_n, -\tau$. We therefore choose the positive sign. For the nuclear spin size we will only consider the noninteger cases $I = \frac{1}{2}, \frac{3}{2}, \frac{5}{2}$ relevant from Table I. The possible nuclear quadrupolar splitting depends much on the nuclear environment and we assume a range for $|\hat{\Delta}_Q|$ from zero to similar size as the hyperfine parameter ξ_n and possibly of both signs.

With the range of parameters defined we first show the dramatic influence of hyperfine coupling on the ordering temperature which is presented by the phase boundary diagram in the (ξ_e, T) plane in Fig. 1. For vanishing hyperfine coupling there is a QCP for the intersite-exchange induced moment order at $\xi_e = 1$ and $T_m(\xi_e)$ collapses with a logarithmic singularity [3] at this point leading to a paramagnetic state for $\xi_e < 1$. Turning on a finite hyperfine coupling to the nuclear spins removes the QCP and the ordering temperature stays finite though small for all $\xi_e < 1$ with a smooth crossover between the two regions. Naturally an increasing nuclear spin size leads to an increased T_m for fixed ξ_n . This is also true when keeping spin size fixed and increasing ξ_n . For $\xi_e \rightarrow 0$ the ordering is dominated by the hyperfine coupling and the limiting value of T_m is given by Eq. (16). Considerably above the QCP the hyperfine coupling has little influence on $T_m(\xi_e)$ which is intersite-exchange dominated in this regime.

The temperature dependence of the two (normalised) order parameters below the transition temperature are shown in Fig. 2 for two typical control parameters above (a) and below (b) the QCP. In the former case the transition at T_m is CEF exchange dominated and $\langle S_x \rangle$ already saturates before the nuclear moment $\langle I_z \rangle$ becomes sizeable only below a temper-

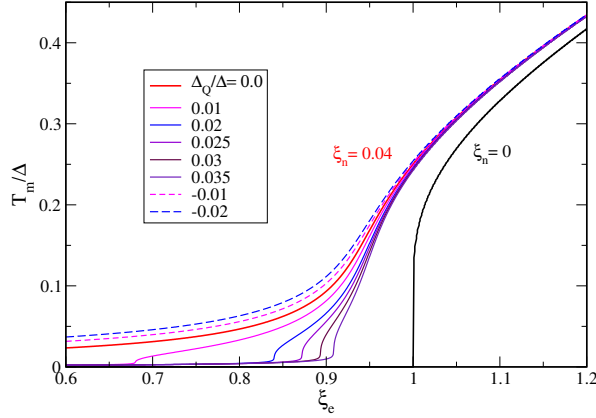


FIG. 11. Ordering temperature as function of ξ_e for various nuclear quadrupole splitting constants $\hat{\Delta}_Q = \Delta_Q/\Delta$. The black curve is the reference for zero hyperfine coupling ξ_n with the QCP at $\xi_e = 1$, all other curves with $\xi_n = 0.04$. Negative Δ_Q enhances the hyperfine dominated transition temperature T_m while positive Δ_Q suppresses T_m (but never reduces to zero), in accordance with Fig. 12.

ature T^* comparable to the nuclear spin splitting induced by $\langle S_x \rangle$. Therefore the temperature dependence of both order parameters in Fig. 2(a) has a rather asymmetric appearance. This is in contrast to Fig. 2(b) for below-critical ξ_e where the ordering at much lower temperature (Fig. 1) is dominated by the hyperfine coupling. In this case the nuclear and electronic moments evolve simultaneously below T_m . The phase diagram in the ξ_e -T plane of Fig. 1 has been obtained from the singularity of the paramagnetic RPA susceptibility in Eq. (12). It is also instructive to follow the evolution of the latter in the ordered regime. We consider the non-critical *homogeneous* susceptibility for the AFM state according to Eq. (27). In the electronic induced moment regime for ξ_e considerably above the QCP it exhibits the typical AFM cusp at T_m and then falls off at lower temperature. For absent hyperfine coupling $\xi_n = 0$ it would saturate [3] at a finite value $(m_s^2/2\Delta)[\xi_e(\xi_e^2 + 1)]^{-1}$ at low temperature, unlike the longitudinal susceptibility in a Kramers degenerate ground state magnet which tends to zero there. In the low temperature region around T^* of Fig. 3 we notice an additional depression which is due to the hyperfine coupling to the split nuclear spin states. When ξ_e is below the QCP value the cusp at T_m is diminished and has moved to the hyperfine dominated regime around T^* where it is still weakly visible. Thus in both cases the hyperfine coupling should lead to a depression of the homogeneous susceptibility in the low temperature ordered regime.

The zero-field specific heat of the model (Sec. V) is shown in Fig. 4(a) for $I = \frac{5}{2}$. It exhibits three superposed anomalies: i) the broad Schottky anomaly around T_{max} due to the two-singlet splitting ii) the jump at the induced ordering temperature T_m for $\xi_e > 1$ above the QCP value. iii) the nuclear specific heat peak at a temperature scale $T^* \approx \xi_n \Delta$ that reflects the splitting of nuclear spin states mediated by the hyperfine coupling to the electronic states. As the electronic

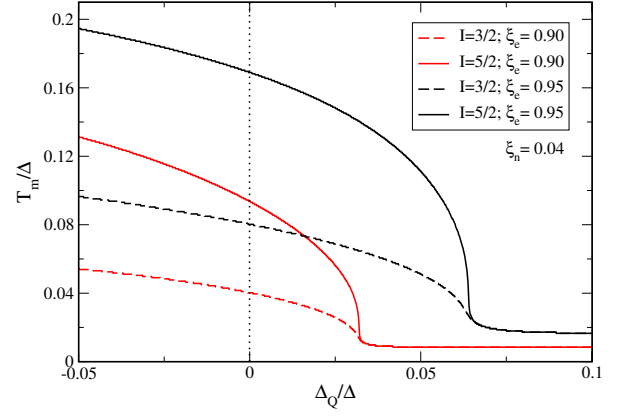


FIG. 12. Dependence of ordering temperature T_m on the nuclear quadrupole coupling constant in the hyperfine interaction dominated regime with subcritical $\xi_e < 1$. The quadrupolar interaction tunes the effective Curie constant of the nuclear spin susceptibility and thus changes the ordering temperature T_m .

control parameter is decreased through the QCP T_m shifts to lower temperatures (cf. Fig. 1) and the specific heat jump is diminished. Finally for $\xi_e < 1$ the ordering appears a much lower temperature $T_m \approx T^*$ dominated by the hyperfine coupling and the jump at the ordering temperature appears inside the nuclear specific heat peak increasing again for lowering ξ_e (in Fig. 4(b)). This intricate crossover appearance of the zero-field specific heat of Fig. 4 is also reflected in the inset of (b) which demonstrates explicitly the nonmonotonic evolution of the specific heat jump across the QCP region. Furthermore the dependence of specific heat anomalies on the nuclear spin I is shown in Fig. 5 for $\xi_e > 1$. The jump at T_m is only weakly affected while the nuclear part at T^* is strongly reduced by the smaller entropy release for decreasing I.

The associated entropy dependence on temperature is shown in Fig. 6 on the two sides of the QCP. As mentioned before for $\xi_e > 1$ part of the entropy release at high temperature happens through excited singlet depopulation as well as through the induced order at T_m and at low temperature the nuclear entropy is released via the nuclear spin splitting caused by the induced order parameter. For subcritical $\xi_e < 1$ there is no more entropy release at T_m and a clear plateau appears after the nuclear entropy has reached saturation $S_n = \ln(2I + 1)$ above the now hyperfine dominated ordering around $T_m \approx T^*$.

A further interesting aspect of the interplay of the three types of specific heat anomalies is their evolution with applied field. In the model calculation only the Zeeman term for CEF singlets has been included due to $\mu_n \ll \mu_B$ but the nuclear spins are indirectly influenced via the hyperfine coupling to the electronic order parameters $\langle S_x \rangle_\lambda$ that depend on the field. The results for the field dependence for FM and AFM exchange coupling and below- and above- critical ξ_e are shown in the four panels of Fig. 7. In the subcritical regime (a,c) the broad Schottky anomaly shifts to higher temperature for FM while it is mostly unaffected for AFM. The nuclear peak around the temperature T^* broadens in the FM case while it

narrows in the AF case. This behaviour is caused by the quite different dependence of order parameters $\langle S_x \rangle_\lambda$ and $\langle I_z \rangle$ on field strength and is also observed in the above-critical region of ξ_e (b,d). The higher temperature electronic part of the specific heat is much different in the FM and AFM cases [6]. The jump at T_m is quickly broadened and shifted to higher temperature for the FM case. On the other hand for AFM case the induced ordering and the associated specific heat jump prevails in finite field but is progressively suppressed in higher fields up to the critical field [6] thus approaching the subcritical appearance of the specific heat in (c).

The specific heat demonstrates that the FM transition changes to a gradual crossover in a finite field because there is no more symmetry breaking involved. On the other hand the AFM transition persists up to a critical field. The corresponding H-T phase diagram as defined by the field dependence of the critical temperature is shown in the two panels of Fig. 8. As mentioned before it is obtained by identifying the field strength where the staggered order parameter $M_s(T, h)$ vanishes. Fig. 8 demonstrates a reentrance behaviour of the AFM magnetic transition temperature, most pronounced above the critical ξ_e . This corresponds to a nonmonotonic dependence of the critical field (the phase boundary) on temperature. It is caused by the rapid change of the electronic and nuclear order parameters and their coupling close to the critical field. This is demonstrated in the two panels of Fig. 9, both referring to the right panel of Fig. 8, which directly show the nonmonotonic shifting of the critical field with temperature. Equivalently the temperature dependence at fixed large field $h' = 0.85$ in the nonmonotonic region as shown in Fig. 10 clearly demonstrates the reentrance signature of magnetic order as witnessed in particular by the staggered order parameter $M_s(T)$ (red dashed) and its nuclear equivalent (right panel) in this figure. We note that this kind of reentrance caused by hyperfine coupling is seen experimentally in a singlet ground state Pr-skutterudite compound [23]. The details of the ordering are different for this compound because its low lying CEF states are of singlet-triplet type rather than two singlets. In fact it has also been observed in Yb- compound with Kramers doublet ground state [11] where it has been attributed to the influence of hyperfine coupling.

Finally we discuss the effect of possible quadrupole splitting of nuclear spin states on the (zero-field) magnetic phase transition. It is of foremost interest how the phase boundary changes with the size of the quadrupolar nuclear coupling constant, in particular around the QCP. This is shown in Fig. 11 with the critical temperature curves obtained from solving Eq. (37). The full red curve gives the reference for zero quadrupolar potential Δ_Q under the presence of finite hyperfine coupling $\xi_n = 0.04$. An increasing (positive) Δ_Q leads to a rapid characteristic suppression of subcritical $T_m(\xi_e)$, but never quite to zero. For above critical ξ_e it has little influence. The overall shape of the critical temperature curve for the large Δ_Q values approaches that of the reference curve for zero hyperfine coupling (full black line). In contrast, for negative quadrupolar coupling constants T^* increases

and the shape of the (red) reference curve is preserved. This distinctive influence of nuclear quadrupole splitting is also seen in complementary Fig. 12 which plots directly the Δ_Q dependence for two subcritical ξ_e and two nuclear spin sizes. The reason for the opposite dependence for different signs of Δ_Q was attributed in Sec. VI to the modification of the nuclear Curie-type susceptibility by the quadrupole splittings.

VIII. SUMMARY AND CONCLUSION

In this work we investigated the influence of the hyperfine coupling with nuclear spins on the properties of CEF singlet-singlet induced moment magnets in the context of a highly symmetric Ising-type model that allows a mostly analytical treatment. Furthermore we include the effects of an external field and in particular the influence of nuclear quadrupole potential leading to a splitting of nuclear spin states.

We have shown that the QCP existing in the purely electronic model is suppressed by the hyperfine coupling and replaced by a crossover from electronic exchange CEF induced moment order with large critical temperature T_m to a subcritical regime below the QCP where the order at a much lower T_m is dominated by the hyperfine coupling and comes to lie within the temperature regime of nuclear spin splitting energy.

Furthermore the temperature and field dependence of both electronic and nuclear order parameters in both ordered regimes was calculated showing characteristic differences in their appearance. In particular the specific heat, its temperature, field and control parameter dependence was investigated. It was found that it is determined by the interplay of three anomalies which is also reflected in the entropy release. They correspond to Schottky type anomaly due to upper singlet depopulation, specific heat jump at the induced moment ordering for above critical electronic control parameter and large and narrow nuclear peak due to lifting of nuclear spin degeneracy. The specific heat jump exhibits a pronounced nonmonotonic evolution when crossing the QCP region. The field dependence shows characteristic differences for these anomalies for FM/AFM models and below/above critical control parameter. In particular the nuclear specific heat peak is broadening for the FM case and in contrast shows narrowing in the AFM case, reflecting the distinct field dependence of the order parameters and associated excitation gaps in the two cases. Furthermore the resulting H-T phase diagram was found to exhibit a peculiar reentrance signature connected with nonmonotonic critical field dependence on temperature which becomes more pronounced with increasing hyperfine coupling.

Finally we have studied in detail the effect of a possible nuclear quadrupole coupling which lifts the nuclear spin degeneracy. It was found that a positive quadrupolar potential suppresses the transition temperature curve which becomes similar to the purely electronic curve for large quadrupole coupling. On the other hand the negative quadrupole coupling enhances the ordering temperature and preserves the shape of the phase boundary. This distinct appearance may be traced back to the properties of the pseudo-Curie nuclear spin sus-

ceptibility in the two cases.

The present work provides a solid theoretical framework for the discussion of the influence of nuclear spins with hyperfine

coupling on singlet-singlet induced moment magnetism which may occur in compounds with non-Kramers 4f ions with sufficiently low site symmetry of the crystalline electric field.

[1] N. Majlis, *The Quantum Theory of Magnetism* (World Scientific, Singapore, 2007).

[2] B. Schmidt and P. Thalmeier, Frustrated two dimensional quantum magnets, *Physics Reports* **703**, 1 (2017).

[3] P. Thalmeier and A. Akbari, Induced quantum magnetism in crystalline electric field singlet ground state models: Thermodynamics and excitations, *Phys. Rev. B* **109**, 115110 (2024).

[4] T. Takimoto and P. Thalmeier, Theory of induced quadrupolar order in tetragonal YbRu_2Ge_2 , *Phys. Rev. B* **77**, 045105 (2008).

[5] K. Haule and G. Kotliar, Complex Landau-Ginzburg theory of the hidden order in URu_2Si_2 , *Europhysics Letters* **89**, 57006 (2010).

[6] P. Thalmeier, Magnetocalorics of singlet ground state induced moment magnets, *Phys. Rev. B* **112**, 104417 (2025).

[7] J. Jensen and A. R. Mackintosh, *Rare Earth Magnetism* (Clarendon Press, Oxford, 1991).

[8] A. Steppke, M. Brando, N. Oeschler, C. Krellner, C. Geibel, and F. Steglich, Nuclear contribution to the specific heat of $\text{Yb}(\text{Rh}_{0.93}\text{Co}_{0.07})_2\text{Si}_2$, *physica status solidi (b)* **247**, 737 (2010).

[9] L. Steinke, K. Mitsumoto, C. F. Miclea, F. Weickert, A. Dönni, M. Akatsu, Y. Nemoto, T. Goto, H. Kitazawa, P. Thalmeier, and M. Brando, Role of hyperfine coupling in magnetic and quadrupolar ordering of $\text{Pr}_3\text{Pd}_{20}\text{Si}_6$, *Phys. Rev. Lett.* **111**, 077202 (2013).

[10] J. Knapp, L. V. Levitin, J. Nyéki, A. F. Ho, B. Cowan, J. Saunders, M. Brando, C. Geibel, K. Kliemt, and C. Krellner, Electronuclear transition into a spatially modulated magnetic state in YbRh_2Si_2 , *Phys. Rev. Lett.* **130**, 126802 (2023).

[11] J. Knapp, L. V. Levitin, J. Nyéki, B. Cowan, M. Brando, C. Geibel, K. Kliemt, C. Krellner, and J. Saunders, Magnetic phase diagram of YbRh_2Si_2 : The influence of hyperfine interactions, *Phys. Rev. Res.* **7**, L042043 (2025).

[12] S. Gabani, I. Curlik, F. Akbar, M. Giovannini, and J. G. Sereni, *Hyperfine electro-nuclear coupling at the quantum criticality of YbCu_4Zn* (2025), arXiv:2506.18192 [cond-mat.str-el].

[13] Y. Aoki, T. Namiki, S. R. Saha, T. Tayama, T. Sakakibara, R. Shiina, H. Shiba, H. Sugawara, and H. Sato, f-electron-nuclear hyperfine-coupled multiplets in the unconventional charge order phase of filled skutterudite $\text{PrRu}_4\text{P}_{12}$, *Journal of the Physical Society of Japan* **80**, 054704 (2011).

[14] T. Kitazawa, Y. Shimura, T. Onimaru, S. Tsuchida, K. Kubo, Y. Haga, H. Sakai, Y. Tokiwa, S. Kambe, and Y. Tokunaga, *Paramagnetic electron-nuclear spin entanglement in $\text{HoCo}_2\text{Zn}_{20}$* (2025), arXiv:2510.21158 [cond-mat.str-el].

[15] H. Eisenlohr and M. Vojta, Limits to magnetic quantum criticality from nuclear spins, *Phys. Rev. B* **103**, 064405 (2021).

[16] K. Andres, Combined electron-nuclear magnetic-ordering phenomena in singlet-ground-state systems, *Phys. Rev. B* **7**, 4295 (1973).

[17] T. Murao, Effective nuclear spin Hamiltonian for magnetically ordered singlet ground state system, *Journal of the Physical Society of Japan* **46**, 40 (1979).

[18] M. Kubota, H. R. Folle, C. Buchal, R. M. Mueller, and F. Pobell, Nuclear magnetic ordering in PrNi_5 at 0.4 mK, *Phys. Rev. Lett.* **45**, 1812 (1980).

[19] T. Murao, Magnetism of a nucleus-electron complex system in the vicinity of the threshold, *Journal of the Physical Society of Japan* **50**, 3240 (1981).

[20] H. B. Møller, J. Z. Jensen, M. Wulff, A. R. Mackintosh, O. D. McMasters, and K. A. Gschneidner, Hyperfine interactions, magnetic impurities, and ordering in praseodymium, *Phys. Rev. Lett.* **49**, 482 (1982).

[21] T. Miki, M. Yanaka, M. Nakagawa, D. Kim, O. Ishikawa, T. Hata, H. Ishii, T. Kodama, and Y. Ōnuki, Electrical resistivity anomaly at the nuclear magnetic ordering in a Van Vleck paramagnet PrCu_6 , *Phys. Rev. Lett.* **69**, 375 (1992).

[22] T. Zajarniuk, A. Szewczyk, P. Wiśniewski, M. U. Gutowska, R. Puzniak, H. Szymczak, I. Gudim, V. A. Bedarev, M. I. Pashchenko, P. Tomeczak, and W. Szuszkiewicz, Quantum versus classical nature of the low-temperature magnetic phase transition in $\text{TbAl}_3(\text{BO}_3)_4$, *Phys. Rev. B* **105**, 094418 (2022).

[23] F. Bangma, L. Levitin, M. Lucas, A. Casey, J. Nyeki, I. Broeders, A. Sutton, B. Andraka, S. Julian, J. Saunders, and A. McCollam, *Diverse influences of hyperfine interactions on strongly correlated electron states* (2023), arXiv:2305.17088 [cond-mat.str-el].

[24] M. P. Zic, C. Huan, N. Silva, Y. Li, M. W. Meisel, and I. R. Fisher, *Electro-nuclear quantum phase transition in TmVO_4* (2025), arXiv:2509.11489 [cond-mat.str-el].

[25] P. Santini and G. Amoretti, Crystal field model of the magnetic properties of URu_2Si_2 , *Phys. Rev. Lett.* **73**, 1027 (1994).

[26] P. Thalmeier, Dual model for magnetic excitations and superconductivity in UPd_2Al_3 , *The European Physical Journal B - Condensed Matter and Complex Systems* **27**, 29 (2002).

[27] M. Sundermann, M. W. Haverkort, S. Agrestini, A. Al-Zein, M. M. Sala, Y. Huang, M. Golden, A. de Visser, P. Thalmeier, L. H. Tjeng, and A. Severing, Direct bulk-sensitive probe of 5f symmetry in URu_2Si_2 , *Proceedings of the National Academy of Sciences* **113**, 13989 (2016).

[28] G. Frossati, J. M. Mignot, D. Thoulouze, and R. Tournier, Van Vleck-like electronuclear susceptibility of ^{171}Yb in Au at very low temperature, *Phys. Rev. Lett.* **36**, 203 (1976).

[29] M. Kofu, O. Yamamuro, T. Kajiwara, Y. Yoshimura, M. Nakano, K. Nakajima, S. Ohira-Kawamura, T. Kikuchi, and Y. Inamura, Hyperfine structure of magnetic excitations in a tb-based single-molecule magnet studied by high-resolution neutron spectroscopy, *Phys. Rev. B* **88**, 064405 (2013).

[30] D. Giglberger and S. Penselin, Ground-state hyperfine structure and nuclear magnetic moment of thulium-169, *Zeitschrift für Physik* **199**, 244 (1967).

[31] A. Abragam, *Principles of Nuclear Magnetism* (Oxford University Press, Oxford, 1961).